Geophys. J. Int. (2007) **171,** 223–230 doi: 10.1111/j.1365-246X.2007.03492.x

Traveltime measurements from noise correlation: stability and detection of instrumental time-shifts

L. Stehly,[1,2] M. Campillo[1] and N. M. Shapiro[3]

[1]*Université Joseph Fourier, CNRS, LGIT,* BP 53, 38041 *Grenoble, France. E-mail: lstehly@obs.ujf-grenoble.fr*
[2]*CEA/DASE,* BP 12, 91680 *Bruyères-le-Châtel, France*
[3]*Laboratoire de Sismologie, CNRS, IPGP,* 4 *place Jussieu,* 75252 *Paris Cedex* 05, *France*

Accepted 2007 May 10. Received 2007 May 10; in original form 2006 October 20

SUMMARY

We test the feasibility of using Green's functions extracted from records of ambient seismic noise to monitor temporal changes in the Earth crust properties by repeated measurements at regional distances. We use about 11 yr of continuous recordings to extract surface waves between three pairs of stations in California. The correlations are computed in a moving 1-month window and we analyse the temporal evolution of measured interstation traveltimes. The comparison of the arrival times in the positive and negative correlation time of Rayleigh and Love waves allows us to separate time-shifts associated with any form of physical change in the medium, those resulting from clock drift or other instrumental errors, and those due to change in the localization of the noise sources. This separation is based on the principle of time symmetry. When possible, we perform our analysis in two different period bands: 5–10 and 10–20 s. The results indicate that significant instrumental time errors (0.5 s) are present in the data. These time-shifts can be measured and tested by closure relation and finally corrected independently of any velocity model. The traveltime series show a periodic oscillation that we interpret as the signature of the seasonal variation of the region of origin of the seismic noise. Between 1999 and 2005, the final arrival time fluctuations have a variance of the order of 0.01 s. This allows us to measure interstation traveltimes with errors smaller than 0.3 per cent of the interstation traveltime and smaller than 1 per cent of the used wave period. This level of accuracy was not sufficient to detect clear physical variation of crustal velocity during the considered 11 yr between the three stations in California. Such changes may be more easily detectable when considering pairs of stations more closely located to each other and in the vicinity of tectonically active faults or volcanoes.

Key words: data quality control, noise correlation, seismology, surface waves.

1 INTRODUCTION

It has been recently shown that the time cross-correlation function of seismic ambient noise (Shapiro & Campillo 2004) computed between a pair of distant stations contains, at least partially, the actual Green's function between the two stations (Campillo 2006; Larose *et al.* 2006, and references therein). The emergence of the Green's function is effective only after a sufficient averaging that is provided by random spatial distribution of the noise sources when considering long time-series as well as the scattering of seismic waves on heterogeneities within the Earth crust (Shapiro & Campillo 2004; Sabra *et al.* 2005b).

Traveltime measurements of Rayleigh waves reconstructed from the seismic noise has been used to produce high resolution regional scale images of the crustal structure in California (Sabra *et al.* 2005a; Shapiro *et al.* 2005). This region is characterized by strong contrasts in seismic velocities within the crust and, therefore, was a relatively easy task for the seismic imaging because the existing anomalies could be well imaged even when using relatively rough traveltime measurements. However, further applications require a more careful analysis of the measurement errors. For example, Green's functions extracted from records of ambient seismic noise can be used for monitoring temporal changes in the Earth crust properties by repeated measurements at regional distances. In this case, the noise-based measurements should be accurate enough to allow us to detect relatively small time-shifts associated with the structural changes. Our goal here is to assess the accuracy of the Green's function reconstructed by cross-correlation of ambient seismic noise and to determine to what extents the noise-based traveltime measurements can be used to detect and to quantify station instrumental errors and to monitor changes in the physical properties of the medium.

High precision measurements of changes of medium properties are possible using repeated analysis of seismic records (e.g. Poupinet *et al.* 1984; Snieder 2006), or noise auto-correlation

(Sens-Schönfelder & Wegler 2006; Wegler & Sens-Schönfelder 2007), but this technique cannot be used to detect phase shift associated with instrumental dysfunction.

We use 11 yr of continuous records to extract the surface waves part of the Green's function between three pairs of stations in California by computing cross-correlations of ambient seismic noise in a moving 1 month window in the two period bands: 5–10 and 10–20 s. We evaluate the apparent traveltime fluctuations of the surface waves for both positive and negative cross-correlation times. The comparison of the traveltimes estimated from positive and negative time surface waves allows us to distinguish the fluctuations due to any form of physical change in the medium from time-shifts resulting from clock drift or other instrumental errors and finally to estimate time errors caused by variations in the distribution of the noise sources.

After presenting data and methods in Section 2, we present results of our analysis in Section 3. First, we analyse traveltime fluctuations measured during a period when no obvious instrumental problem occurred. Then, we consider a different time interval to determine what part of the observed time fluctuation is due to instrumental errors and, finally, we correct the data from the measured instrumental errors.

2 DATA AND METHODS

Our goal is to study the evolution of traveltimes of both Rayleigh and Love waves measured by cross-correlating ambient seismic noise for a given path and period band. In an ideal case when noise sources are distributed homogeneously over the medium, for a pair of stations A and B (Fig. 1) the surface wave arrival time should be identical on the positive (corresponding to wave going from the station A to the station B) and negative correlation time (corresponding to wave going in the opposite direction) as discussed in Lobkis & Weaver (2001), Van Tiggelen (2003), Snieder (2004) and Sánchez-Sesma & Campillo (2006), and should not change with time. However, three main factors can leads to fluctuations.

(i) A physical change in the medium would result in either a faster or slower traveltime measured in both positive and negative cross-correlation time.

(ii) A clock error in one of the two stations would produce a time-shift of the whole cross-correlation resulting in a larger traveltime in the positive time and a smaller apparent traveltime in the negative time or vice versa. A change in the phase of the response of one of the sensors would have the same effect.

(iii) A change in the spatial distribution of the source of the noise should affect the positive and negative correlation time independently, since the positive and negative time are sensitive to noise sources located in different regions (Fig. 1)

The traveltime variation $\delta\tau$ of surface waves reconstructed by cross-correlation of seismic noise with respect to a 'reference traveltime', for a given path and period band can be written:

$$\delta\tau_{ij}(t) = D(t) + \varphi(t) + \varepsilon(t)_{ij}. \quad (1)$$

In this equation $\delta\tau(t)$ denotes the variation of surface wave traveltime measured either on the positive or on the negative part of the cross-correlation. *ij* is the couple of components of the noise records which are correlated (either Z, R or T). For example, $\delta\tau_{ZR}(t)$ represents the variation of the arrival time of surface waves measured on the the cross-correlation computed between vertical and radial components. D is the time delay caused by a relative drift of the two station clocks (or a phase shift of the sensor response). φ is the time-shift due to a change in the medium. D is an even function where as φ is an odd function: a relative drift of the two station clocks would result in shorter arrival time in the negative time of the cross-correlation, and larger arrival time in the positive time or vice versa. This property was used in marine acoustics (Sabra *et al.* 2005c). On the other hand, a change in the medium would result in either shorter or larger arrival time in both negative and positive time. ε_{ij} is the time-shift due to a change in the spatial distribution of the source. This last term is expected to decrease when increasing the length of the correlated time-series because of the better spatial homogenization of the distribution of noise sources.

By taking the even and odd part of the eq. (1), we obtain:

$$\frac{\delta\tau_{ij}(t) + \delta\tau_{ij}(-t)}{2} = D(t) + \frac{\varepsilon_{ij}(t) + \varepsilon_{ij}(-t)}{2} \quad (2)$$

$$\frac{\delta\tau_{ij}(t) - \delta\tau_{ij}(-t)}{2} = \varphi(t) + \frac{\varepsilon_{ij}(t) - \varepsilon_{ij}(t)}{2}. \quad (3)$$

These two equations would enable us to evaluate surface wave traveltime variations due to a change in the medium φ and to the relative drift of the station clock D, under the assumption that D and φ are large compared to $\frac{\varepsilon_{ij}(\tau) \pm \varepsilon_{ij}(-\tau)}{2}$.

Two strategies can be used to evaluate D and φ.

(i) By using cross-correlation of 'small' time window (1 month) one can evaluate the drift with an accurate time resolution. But with such a time window we expect that the term ε to be quite large, so only large instrumental errors can be evaluated.

(ii) By using cross-correlation of a larger time windows, we degrade the time resolution, but we expect the term ε to be smaller. Therefore, smaller long term instrumental drifts or physical changes of the medium can be identified more easily.

2.1 Data used

We analyse the fluctuations of the apparent traveltime of Rayleigh and Loves waves reconstructed by cross-correlating seismic ambient noise, by using 11 yr (1991–1996 and 1999–2005) of continuous records on three components at three Californian stations: GSC, PFO and PAS (see Fig. 2).

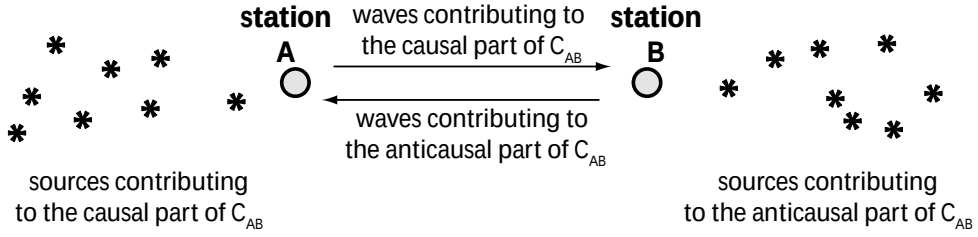

Figure 1. Schematic representation of reconstruction of the causal and the anticausal parts of Green's function from the noise.

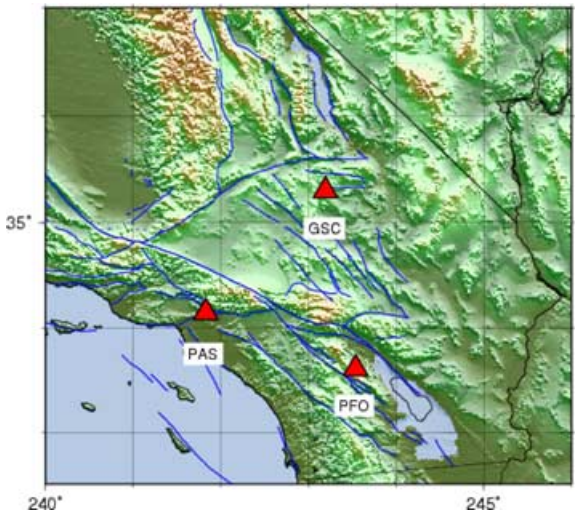

Figure 2. Map of Southern California showing the location of the 3 broadband stations used for this study.

Before computing the cross-correlations, records were corrected from the instrumental response and bandpassed either between 5 and 10 s or between 10 and 20 s. To reduce the contribution of the most energetic arrivals, we disregarded completely the amplitude and considered one-bit signals only (Campillo & Paul 2003; Shapiro & Campillo 2004). Horizontal components records were rotated to radial and transverse directions assuming the propagation along the interstation great circle. We correlated the signal recorded on the components that correspond to non-zero term of the Green's function (ZZ, TT, ZR, RZ and RR). Correlations of 1-d records are then stacked month per month or 6 months per 6 months.

2.2 Measurement of the time delay

First, we define a 'reference Green's function' (RGF) for every path in two period bands (5–10 and 10–20 s) and for all components (ZZ, TT, ZR, RZ and RR) by computing the one-bit cross-correlations of 6 yr (1999–2005) of continuous records of seismic noise. This period was used because we found that no major instrumental errors occurred during these years for any of the three stations considered. The ZZ component of RGF for the path GSC-PAS in the 10–20 s period band is shown on Fig. 3. This waveform is not perfectly symmetric: the amplitude of the Rayleigh waves is larger for the anticausal part than for the causal part of the cross-correlation. This means than in average, between 1999 and 2005, more energy propagates from PAS to GSC than from GSC to PAS (Van Tiggelen 2003; Paul *et al.* 2005; Pedersen *et al.* 2006; Stehly *et al.* 2006). We can also notice that the shapes of the causal and the anticausal signals are quite different because the spectrum of the noise travelling from GSC to PAS and from PAS to GSC differs as well. We however checked that the two wavetrains are associated with the same dispersion curve.

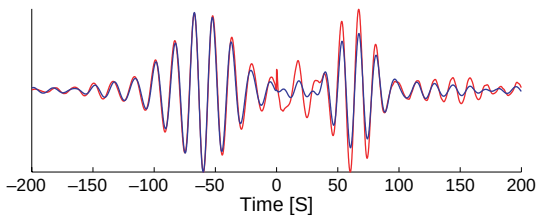

Figure 3. Reference Z–Z cross-correlation for GSC-PAS filtered between 10 and 20 s (grey solid line, red in the online version) and cross-correlation of 2000 May (black dashed line, blue in the online version). Amplitude are normalized to 1.

Once the RGFs are defined for all paths, bandwidths and components, we computed cross-correlations for all 30 d periods during 11 yr (1991–1996 and 1999–2005). For every window, we compare the arrival time of the surface wave of the current month, with the reference for both the causal and anticausal parts. The variation of traveltime are measured from the phase of the cross-spectrum computed between the RGF and the Green's function estimated in the current window.

To obtain more robust traveltime measurements, we limit our analysis to period bands close to two main microseismic peaks at 7 and 14 s that dominate the noise spectrum. At these periods, the sensitivity of Rayleigh waves to the medium maximizes at approximate depths of 6 and 12 km, respectively. To determine what part of the frequency band is usable, we divide our original frequency band in several narrow-bands (8 for the cross-correlations computed between 10–20 and 16 between 5 and 10 s). In every narrow frequency band, we compute the spectral phase difference between the RGF and the current Green's function as a function of frequency and use a linear regression to evaluate the apparent time delay. We consider that a measurement is valid if the variance is smaller than a given threshold. This threshold corresponds to 0.003 s when processing data in the 5–10 s period band and 0.01 s when considering data in the 10–20 s period band. In the following, we take in account only those narrow frequency-bands where this requirement is fulfilled for the entire 11 yr of data. The measurement on each of these subbands is then averaged to obtain the final apparent delay for the 5–10 and 10–20 s period bands. Note that the phase differences are always measured at the same frequencies. Therefore, measured traveltime variations are not affected by changes in the spectrum of the noise. We average the time delay measured with ZZ, ZR, RZ and RR correlations that we consider to be consisting mostly of Rayleigh waves. We also compute a time delay associated with Loves wave by considering TT correlations.

In average, when considering a single component, 33 per cent of the period band correlated is actually used to measure the time delay. However, when we average the measured time delay over the components, we use 70 per cent of the period band correlated because the measurement is not performed exactly on same periods for the ZZ, ZR, RZ, RR and TT correlation.

3 RESULTS

Fig. 4(a) shows the variation of the arrival time of Rayleigh (left-hand panel) and Love (right-hand panel) waves for GSC-PAS in the 5–10 s period band. Measurements performed in the positive time of the correlation are in blue, and those performed in the negative time are in red on the same scale. The positive part of the correlation corresponds to waves travelling from GSC to PAS while the negative time corresponds to waves travelling from PAS to GSC. Two main periods can be distinguished. Between 1991 and 1996, the apparent arrival times exhibit large fluctuations that can be up to 2 s. We remark that the same main features of the time delay can be seen for the averaged Rayleigh and Love waves measurements. Between 1999 and 2005, arrival times are very stable and their fluctuations do not exceed 0.2 s. The fluctuations are systematically much larger for the positive time. Let us first consider the 1999–2005 period.

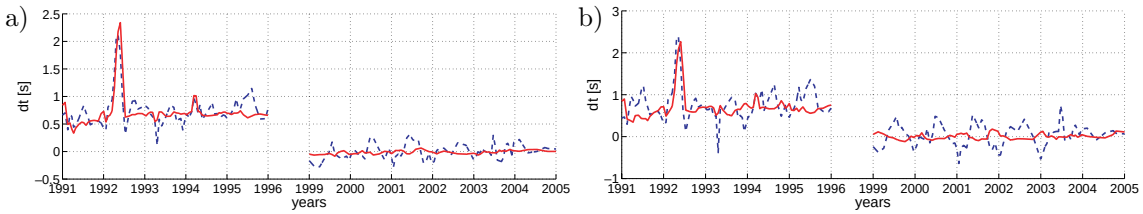

Figure 4. Traveltime variations of Rayleigh (a) and Love (b) waves, for the path GSC-PAS measured from 1-month cross-correlations in the 5–10 s period band. Traveltime of Rayleigh waves are obtained by averaging measurements performed on Z-Z, Z-R, R-Z and R-R cross-correlations. Loves waves are obtained from T-T cross-correlations. Results from the positive and negative correlation time are shown with dashed and solid lines, respectively.

3.1 Time delay in the 5–10 s period band between 1999 and 2005

We consider the period 1999–2005, for which we did not detect any obvious instrumental errors. Fig. 5 shows the apparent traveltime variations of surface waves for paths GSC-PAS, GSC-PFO and PAS-PFO in the 5–10 s period band, averaged over all components of the Green's function, that is including both Love and Rayleigh waves. The correlations are performed day per day and are then stacked month per month using a moving window. Results from the positive time of the correlation shown with a blue line correspond to waves going from the first to the second station (i.e. from GSC to PAS, GSC to PFO and PAS to PFO). The red line shows results from the negative part of the cross-correlations.

The negative time of the correlation of GSC-PAS is sensitive to sources located in the Pacific Ocean and exhibits smaller fluctuations than the positive time which is sensitive to sources in the Atlantic Ocean (Stehly *et al.* 2006). The fluctuations on the negative time of GSC-PAS never exceed 0.05 s and has a variance of only 0.0007 s.

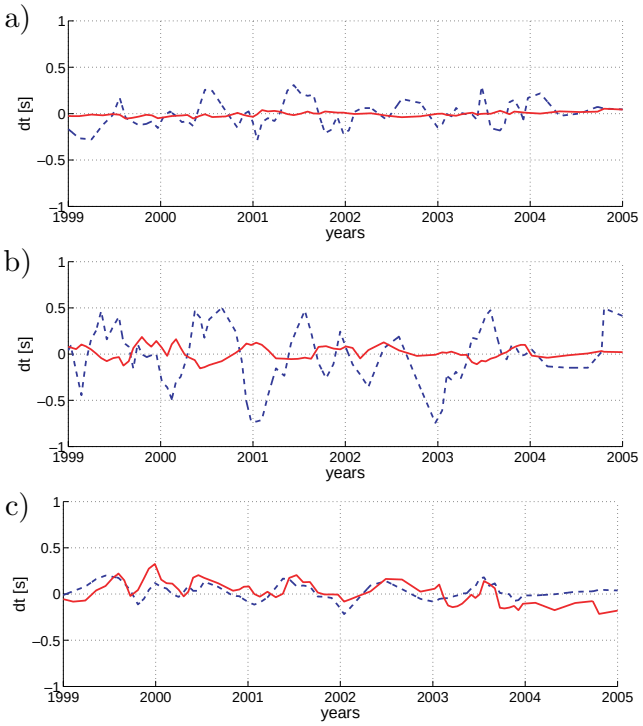

Figure 5. Variation of the surface waves traveltimes measured in the period band 5–10 s and averaged on all components for different paths: (a) GSC-PAS, (b) GSC-PFO and (c) PAS-PFO. Results obtained from positive and negative cross-correlations time are shown with dashed and solid lines, respectively.

As the traveltime of the Rayleigh waves is about 60 s, the maximum amplitude of the fluctuations and its variance represents, respectively, 0.08 and 0.0012 per cent of the traveltime of the Rayleigh waves. This shows that the reconstruction of the Green's function is extremely robust. Also, the equal traveltimes measured from the negative and positive time of cross-correlations demonstrate that no significant instrumental errors occurred between 1999 and 2005.

Largest fluctuations are found for the causal part of the GSC-PFO cross-correlation. The Green's function reconstruction is less stable for this path because it is not directed toward a nearly located oceanic coast. However, even for this 'unfavourable' path the observed fluctuations never exceed 0.75 s (i.e. about 1 per cent of the traveltime of Rayleigh waves), for a relatively short windows of analysis of 1 month. Moreover, the fluctuations measured from the negative part are less than 0.19 s (i.e. 0.3 per cent of the traveltime).

3.2 Time delay in the 10–20 s period band between 1999 and 2005

The upper panels of the Fig. 6 shows the traveltime variation of surface waves measured in the 10–20 s period band and averaged on all components. Cross-correlations were computed in a moving 1-month window. Similar to Fig. 5, positive times correspond to waves going from GSC to PAS and from GSC to PFO. We do not show the result for PAS-PFO, because the Green's function for this path is not well reconstructed in the 10–20 s period band.

The location of sources of the background primary microseism (10–20 s period band) is not constant and has a clear seasonal dependence (Stehly *et al.* 2006). As a consequence, the term ε_{ij} in eq. (1) is expected to exhibit significant seasonal oscillations. This can be clearly seen in the measured traveltimes that exhibit clear fluctuations with a nearly 1-yr period whose amplitude reaches 0.5 s for both paths and for the causal and the anticausal parts of cross-correlations simultaneously. These fluctuations prevent us from achieving a satisfactory accuracy from cross-correlating only 1 month of data in the 10–20 s period band. To have a more stable Green's function reconstruction, we should use longer time windows.

The lower panels of Fig. 6 shows the variations of the arrival time of surface waves when considering cross-correlation over a moving window of 6 months. These variations never exceed 0.2 s for the GSC-PAS path (0.3 per cent of the traveltime) and 0.16 s for the GSC-PFO path (0.25 per cent of the traveltime). These values represents about 1 per cent of the central period of the signal.

3.3 Evidence of instrumental time-shifts during 1991–1996

3.3.1 Time fluctuation for GSC-PAS

Variations of the arrival time for the path GSC-PAS for the two period bands 5–10 and 10–20 s during the period 1991–1996 are

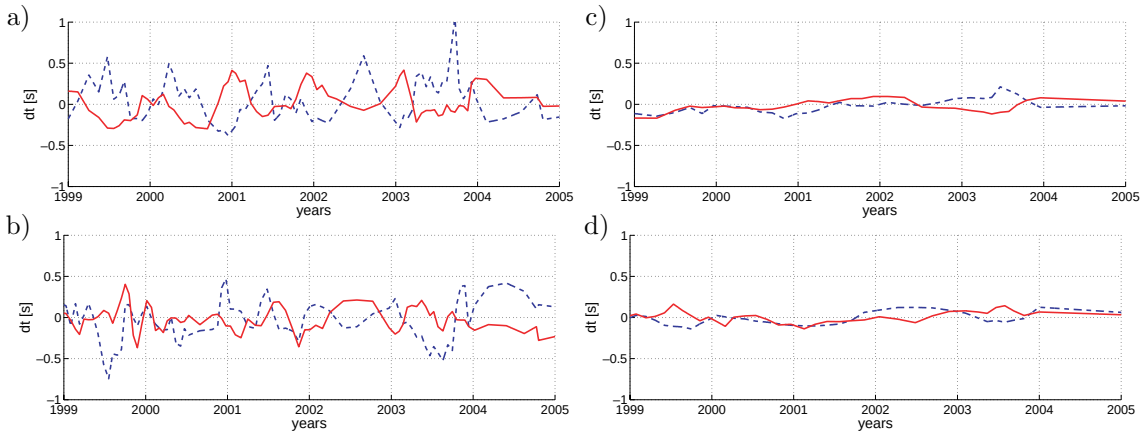

Figure 6. Surface wave traveltime variations measured in the 10–20 s period band and averaged on all components. (a) GSC-PAS using 1 month stacks (b) GSC-PAS using 6 months stacks. (c) GSC-PFO using 1 month stacks (d) GSC-PFO with 6 months stacks. Results obtained from the positive and negative correlation time are shown with dashed and solid lines, respectively.

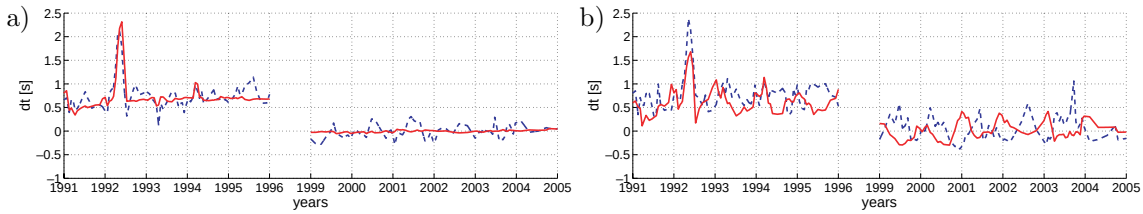

Figure 7. Surface wave traveltime variations averaged on all components for the path GSC-PAS at period ranging from (a) 5 to 10 s (b) 10 to 20 s. Results obtained from the positive and negative correlation time are shown with dashed and solid lines, respectively.

shown in Fig. 7. Averaged relative time delays measured from the positive and negative times of the reconstructed Green's functions are clearly correlated for the two period bands. In 1992, the time delay $\delta\tau(t)$ exhibits a peak reaching 2 s, that can be observe both for positive and negative correlation time with the same polarity. Also a positive time-shift is observed during all the considered period on the positive and negative time. This means that the apparent arrival time become larger on the positive time and smaller in the negative time. These observations cannot be related to changes of the physical properties of the crust that would result in fluctuations of opposite polarity for the positive and negative correlation time (the function $\varphi(t)$ in eq. 1 is an odd function). It is also unlikely that such almost perfectly even variations are due to the variations in the distribution of the microseism sources because the positive and negative cross-correlation times are not sensitive to sources located in the same region (Fig. 1). Moreover, all these features can be seen on the two period bands 5–10 and 10–20 s (Fig. 7b) while the source of noise are not expected to be the same for the two period bands (Stehly *et al.* 2006). Therefore, these even and period-independent time fluctuations strongly suggest a clock drift or instrumental errors at one of the two stations.

3.3.2 Evaluating instrumental errors for the GSC-PAS path

By taking the even part of the surface wave traveltime fluctuations obtained from the positive and negative noise cross-correlation time, we isolate instrumental errors (see eq. 2). Results from the two period bands presented in Fig. 8 show several robust features (i.e. the fluctuations that can be observed in the two period bands simultaneously): the main peak of 1992, the minor peak of 1994, the offset of the curve between 1991–1996 and 1999–2005, as well as the small positive trend between 1991 and 1996. Smaller instrumental errors are masked by the fluctuations associated with changes in the spatial distribution of the noise sources.

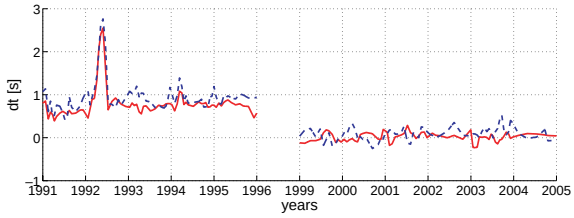

Figure 8. Relative instrumental error between GSC and PAS measured in the 5–10 s (dashed line) and the 10–20 s (solid line) period bands by computing the even part of $\delta t(t)$ following eq. (2).

3.3.3 Comparing observed instrumental errors for different paths

We also evaluate instrumental errors for the GSC-PFO and the PAS-PFO paths during 1991–1996 using a moving 1-month window. For PAS-PFO, we only used the period band 5–10 s because the Green's function is not well reconstructed between 10 and 20 s. We show the results in Fig. 9. Relative instrumental errors for GSC-PFO are similar to those measured for GSC-PAS: the main peak of 1992, the minor peak of 1994 and the shift in the arrival time between 1991–1996 and 1999–2005. These features are not observed for the PAS-PFO path. Therefore, they are likely all caused by instrumental problems at GSC.

One can note that the shape and the amplitude of the 1992 and 1994 peaks are not exactly similar for the two paths: GSC-PAS and

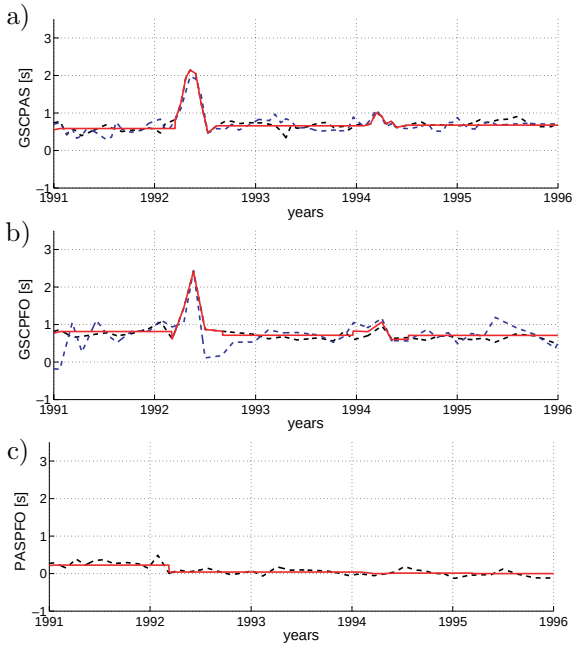

Figure 9. Instrumental errors computed using eq. (2) for different paths: (a) GSC-PAS, (b) GSC-PFO and (c) PAS-PFO. Measurement performed in the 5–10 s period band are shown with a dashed line, and those between 10 and 20 s are shown with a dotted line. In solid line we show the 'schematic' relative instrumental errors defined as following. (i) During the peak of 1992 and 1994, we use the average value of the instrumental errors computed in the period band 5–10 and 10–20 s using 1 month stack. We do not average the measured value overtime. (ii) The rest of the time, we show the 'slowly evolving instrumental error', by taking the average value of the relative clock error evaluated during the three period of time: 1991 January–1992 March, 1992 August–1994 February and 1994 May–1995 December 1995. Again we average measurements performed in the two period bands, 5–10 and 10–20 s. The value used are summed up on Table 1.

GSC-PFO. This apparent discrepancy is explained by the different data availabilities for the two pairs of stations. As a consequence, our measurements are not made exactly at the same dates. Moreover, the amplitude of the 1992 peaks is equal to 2.41 s for GSC-PFO and 2.14 s for GSC-PAS. This suggests there is also a small relative error between PFO and PAS.

3.3.4 Slowly evolving instrumental time-shifts

We exclude the period of the two peaks of 1992 and 1994, and we consider only long term variations of the time delay that are much smaller than the 1992 peaks. One can notice in Fig. 9 that the average values of the measured instrumental error change slightly with time for the three paths. Three main periods can be distinguished:1991–March 1992, August 1992–February 1994, and may 1994–December 1995. We average the measurement performed in 5–10 and 10–20 s period band, in this three main periods to evaluate the long term instrumental errors. For example, for GSC-PAS between 1991 and the beginning of the 1992 peak, the average error is 0.585 s whereas it is 0.65 s between the 1992 and 1994 peaks and 0.67 s after the 1994 peak. This suggests long term drifts of the clock at some of the stations, or others slowly evolving instrumental problems. Measurements of the different average values of the surface wave arrival times measured from the noise correlations are summarized in Table 1. We can check that they actually correspond to

Table 1. Average values of the relative instrumental errors for three stations pairs: GSC-PAS, GSC-PFO and PAS-PFO computed with eq. (2) from moving stacks of 1 month of cross-correlations of ambient seismic noise, performed in the two period band 5–10 and 10–20 s. The three-station closure relation of relative instrumental errors is (GSC-PAS)−(GSC-PFO)+(PAS-PFO).

	1991–1992	1992–1994	1994–1996
GSC-PAS	0.585	0.658	0.675
GSC-PFO	0.814	0.714	0.709
PAS-PFO	0.226	0.041	0.013
Closure	−0.0018	−0.014	−0.02

a relative instrumental errors of the stations, by verifying a closure relation. The relative instrumental error of GSC-PAS - GSC-PFO + PAS-PFO should be equal to zero. Observed closure amplitudes are smaller than 0.02 s which is one order of magnitude smaller than the measured long term instrumental errors.

3.3.5 Evaluating station time-shifts from relative time-shifts measurements

In the previous sections, we evaluated the relative instrumental errors between pair of stations. The next step is to obtain the absolute instrumental errors at each stations. Obtaining individual station errors from relative measurements is not straightforward, and has not a unique solution: The relative clock error of GSC-PAS, GSC-PFO and PAS-PFO give us three equations, but only two of them are independent whereas we have three unknowns: the error at GSC, PAS and PFO. Concerning the major dysfunctions (the peaks of 1992 and 1994), we have already seen that they are all due to a problem at GSC as seen on Section 3.3.3.

For the slowly evolving errors, although several scenarios could fit our measurements, we propose the following model under the arbitrary assumption that there is no error on PAS (this subjective hypothesis is only considered to check how consistent are our measurements):

(i) Between 1991 and the beginning of the peak of 1992 (see Table 1), GSC has error equal to 0.58 s, PFO an error of about 0.23 s, and PAS no error at all. This would explain that the relative error for the GSC-PAS path is 0.58 s, the one for GSC-PFO is 0.81 s and for PAS-PFO it is equal 0.23 s.

(ii) Between the peaks of 1992 and 1994: GSC has an error of +0.65 s and PFO has an error of −0.056 s.

(iii) between 1994 and 1996, GSC would have an error of +0.67 s and PFO an error of −0.03 s.

Our evaluation of individual station errors are summarized in Table 2.

Table 2. Interpretative values of instrumental errors for the stations GSC and PFO, under the assumption that there is no error at PAS and deduced from the measurements of relative instrumental errors of GSC-PAS, GSC-PFO, and PAS-PFO.

	1991	1992	May 1992	1993	1994	April 1994	1995
GSC	+0.58 s		+2.18 s	+0.65 s		+1.00 s	+0.67 s
PFO	−0.23 s			−0.056 s		−0.06 s	−0.03 s
PAS	+0 s						

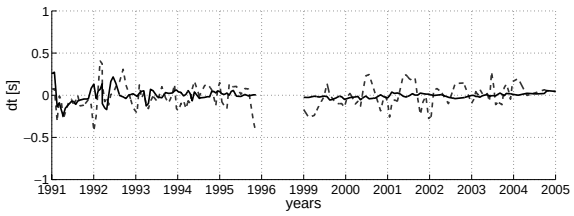

Figure 10. 5–10 s surface wave traveltime variations averaged on all components for the GSC-PAS path after correcting the instrumental errors shown on Fig. 9. Results obtained from the positive and the negative correlation times are shown with dashed and solid lines, respectively.

3.3.6 Correcting instrumental time-shifts

After evaluating the instrumental errors $D(t)$ (see eq. 2, and Fig. 9), we remove them from the data. Fig. 10 presents the traveltime variations remeasured for the GSC-PAS path between 5 and 10 s after removing the estimated instrumental errors. We corrected the data from the average peak of 1992 and 1994 measured in the 5–10 and 10–20 s period band, using stack of 1 month of cross-correlation, as well as the slowly evolving error evaluated by taking the average value of the time delay $\delta\tau(t)$ for the three periods 1991–1992, 1992–1994 and 1994–1996. This corresponds to the instrumental errors shown in red on Fig. 9, and to the value in Tables 1 and 2.

Following eqs (1) and (2), the measured time delay fluctuations $\delta\tau^*$ after correcting the data from the instrumental errors are:

$$\delta\tau^*_{ij}(t) = [D(t) + \varphi(t) + \varepsilon_{ij}(t)] - \left[D(t) + \frac{\varepsilon_{ij}(t) + \varepsilon_{ij}(-t)}{2}\right] \quad (4)$$

$$\delta\tau^*_{ij}(t) = \varphi(t) + \frac{\varepsilon_{ij}(t) - \varepsilon_{ij}(-t)}{2}, \quad (5)$$

φ is the time-shift due to a change in the medium and ε is the time-shift due to a change in the spatial distribution of the sources of noise.

The peaks of 1992 and 1994 have completely disappeared as expected, as well as the time-shift between the 1991–1996 and 1999–2005 period and the small trend between 1991 and 1996 (Fig. 10).

The measured time delay in the positive and negative time of the cross-correlation are not correlated (Fig. 10). In other words after correction of the instrumental errors, $\delta\tau^*$ is not an odd function, whereas φ is an odd function (see Section 2). This means that in eq. (4), φ is small with regard to $\frac{\varepsilon_{ij}(t)-\varepsilon_{ij}(-t)}{2}$. Therefore, we could not detect any change of the medium and the fluctuations of the remeasured time delay are mainly due to changes in the spatial distribution of the noise sources.

Traveltime fluctuations after the correction of instrumental errors have a variance of 0.012 and 0.0022 s on the positive and negative time, respectively. This represents 0.02 and 0.003 per cent of the traveltime of Rayleigh waves. This shows that the Green's functions reconstructed by correlating ambient seismic noise are accurate enough to detect and to correct small instrumental errors and to measure interstation traveltimes with a precision of a few tenths of second for stations 200 km apart.

4 CONCLUSIONS

We studied variations of surface wave traveltimes measured from cross-correlations of seismic noise records between three seismic stations in California during 11 yr in two period bands: 5–10 and 10–20 s. Simultaneous analysis of causal and anticausal parts of cross-correlations allowed us to isolate and to correct various instrumental time-shifts occurred between 1991 and 1996. This measure of instrumental error does not require any assumption on the wave velocity and relies only on the fundamental properties of time symmetry. It could be used routinely to detect instrumentals problems.

Remaining traveltime fluctuations were attributed to errors caused by variations in distribution of the noise sources. In the 10–20 s period band, these errors exhibit strong fluctuations with a clearly identified 1-yr period that is related to seasonal migration of sources of the primary microseism (Stehly *et al.* 2006). These seasonal fluctuations can be reduced by averaging the results in longer time windows.

After introducing all discussed corrections, the interstation traveltimes can be measured with a precision of a few tenths of a second for stations separated by ∼200 km. The achieved level of accuracy was not sufficient to unambiguously detect traveltime variations associated with changes of the physical properties of the crust for the three station pairs and during the considered 11 yr. The obtained results are, however, encouraging because they demonstrated that the traveltime variations can be measured with errors that are smaller than 0.3 per cent of the interstation traveltime and than 1 per cent of the considered wave period. First, this indicates that the precision of the measurement is at least comparable with the one obtained with earthquakes implying that the noise correlation is definitely a good approach for high resolution seismic imaging. Second, the noise based traveltime measurements over shorter paths are expected to be more sensitive to localized changes in the media. Therefore, for future experiments we suggest to consider pairs (or arrays) of stations separated only by a few tens of kilometres up to one hundred of kilometres and located very close to tectonically active features such as active faults or volcanoes. With such configurations the achieved absolute level of accuracy of the noise-based traveltime measurements that can be achieved may be sufficient to detect variations of the physical properties of the crust caused by tectonic or volcanic processes. Using surface waves extracted from the noise in the microseismic peak frequency bands will allow us to monitor relatively deep parts of the crust where it is very difficult to obtain repeatable measurements based on artificial seismic sources.

ACKNOWLEDGMENTS

This work does not intend by any way to criticize the important work that has been done by the researcher and engineers who developed instruments and networks which recorded the data used in this work and to which they generously give an open access to the community. All the seismic data used in this study have been obtained at the IRIS DMC (http://www.iris.edu/), and comes from the Southern California Seismic Network.

This research has been supported by the Commissariat à l'Energie Atomique (CEA, France), by the Agence National de la Recheche (France) under contract PrecorSis (05-CATT-010-01) and CoherSis, and by the European Community (project Neries).

REFERENCES

Brenguier, F., Shapiro, N.M., Campillo, M., Nercessian, A. & Ferrazzini, V., 2007. 3D surface wave tomography of the Piton de la Fournaise Volcano using seismic noise correlations, *J. geophys. Res.*, **34,** L02305, doi:10.1029/2006GL028586.

Campillo, M., 2006. Phase and correlation in 'random' seismic fields and the reconstruction of the Green's function, *Pure appl. Geophys.*, **163,** 475–502.

Campillo, M. & Paul, A., 2003. Long-range correlations in the diffuse seismic coda, *Science*, **299,** 547–549.

Larose, E. *et al.*, 2006. Correlation of random wavefields: an interdisciplinary review, *Geophysics*, 71(4).

Lobkis, O. & Weaver, R., 2001. On the emergence of the Green's function in the correlations of a diffuse field, *J. acoust. Soc. Am.*, **110,** 3011–3017.

Paul, A., Campillo, M., Margerin, L., Larose, E. & Derode, A., 2005. Empirical synthesis of time-asymmetrical Green's functions from the correlation of coda waves, *J. Geophys. Res. (Solid Earth)*, **110,** 8302, doi:10.1029/2004JB003521.

Pedersen, H., Krüger, F. & the SVEKALAPKO Seismic Tomography Working Group, 2006. Influence of the seismic noise characteristics on noise correlations in the baltic shield, submitted.

Poupinet, G., Ellsworth, W. & Frechet, J., 1984. Monitoring velocity variations in the crust using earthquake doublets: an application to the calaveras fault, california, *J. geophys. Res.*, **89,** 5719–5731.

Sabra, K., Gerstoft, P., Roux, P., Kuperman, W.A. & Fehler, M.C., 2005b. Extracting time-domain Green's function estimates from ambient seismic noise, *Geophys. Res. Lett.*, **32,** doi:10.1029/2005GL023155.

Sabra, K., Gerstoft, P., Roux, P. & Kuperman, W., 2005a. Surface wave tomography from microseisms in southern California, *Geophys. Res. Lett.*, **32,** doi:10.1029/2005GL023155.

Sabra, K., Roux, P., Thode, A. G., D'Spain, Hodgkiss, W. & Kuperman, W., 2005c. Using ocean ambient noise for array self-localization and self-synchronization, *J. Seismol.*, 30(2).

Sánchez-Sesma, F. & Campillo, M., 2006. Retrieval of the Green's function from cross correlation: the canonical elastic problem, *BSSA*, in press.

Sens-Schönfelder, C. & Wegler, U., 2006. Passive image interferometry and seasonal variations of seismic velocities at Merapi Volcano, Indonesia, *Geophys. Res. Lett.*, **33,** L21302, doi:10.1029/2006GL027797.

Shapiro, N. & Campillo, M., 2004. Emergence of broadband rayleigh waves from correlations of the ambient seismic noise, *Geophys. Res. Lett.*, **31,** doi:10.1029/2004GL019491.

Shapiro, N., Campillo, M., Stehly, L. & Ritzwoller, M., 2005. High-resolution surface wave tomography from ambient seismic noise, *Science*, **307,** 1615–1618.

Snieder, R., 2004. Extracting the Green's function from the correlation of coda waves: a derivation based on stationary phase, *Phys. Rev. E*, **69**.

Snieder, R., 2006. The theory of coda wave interferometry, *Pure appl. Geophys.*, **163,** 455–473.

Stehly, L., Campillo, M. & Shapiro, N., 2006. A study of the seismic noise from its long range correlation properties, *J. geophys. Res.*

Van Tiggelen, B., 2003. Green's function retrieval and time reversal in a disordered world, *Phys. Rev. Lett.*, 91(24).

Wegler, U. & C., Sens-Schönfelder, 2007. Fault Zone Monitoring with Passive Image Interferometry, *Geophys. J. Int.*, in press.